

IMPROVED PENALTY ALGORITHM FOR MIXED INTEGER PDE CONSTRAINED OPTIMIZATION (MIPDECO) PROBLEMS

DOMINIK GARMATTER*, MARGHERITA PORCELLI†, FRANCESCO RINALDI‡, AND
MARTIN STOLL*

Abstract. Optimal control problems including partial differential equation (PDE) as well as integer constraints combine the combinatorial difficulties of integer programming and large-scale systems resulting from discretizing the PDE. A common solution strategy for such a problem would be Branch-and-Bound. In order to provide an alternative solution approach, especially in a large-scale context, this article investigates penalization techniques. Taking inspiration from a well-known family of existing Exact Penalty algorithms a novel Improved Penalty Algorithm is derived. Using a standard stationary model problem, the algorithm is then numerically investigated and compared with different solution strategies including a naive penalty approach and the Branch-and-Bound routine from CPLEX.

Key words. mixed integer optimization, optimal control, PDE-constrained optimization, exact penalty methods

AMS subject classifications. 65K05, 90C06, 90C11, 93C20

1. Introduction. Optimal control problems governed by a partial differential equation (PDE), integer constraints on the control and possible additional constraints are commonly referred to as mixed integer PDE-constrained optimization (MIPDECO) problems. They pose several challenges as they combine two fields that have been surprisingly distinct from each other in the past: integer programming and PDEs. While integer optimization problems have an inherent combinatorial complexity that has to be dealt with, PDE-constrained optimization problems have to deal with possibly large-scale linear systems resulting from the discretization of the PDE, see, e.g., [27].

Albeit these challenges MIPDECO problems are gaining an increased attention as they naturally arise in many real world applications such as gas networks [14, 24], the placement of tidal and wind turbines [9, 29, 28] or power networks [12], and from the theoretical point of view recent advances include a Sum-up-Rounding strategy [21] and a derivative-free approach [15].

A classical solution approach for a MIPDECO problem is to *first-discretize-then-optimize* where the PDE and the control are discretized and therefore the continuous MIPDECO problem is then approximated by a finite-dimensional (and possibly large-scale) mixed-integer nonlinear programming problem (MINLP). Standard techniques, see, e.g., [3] for an excellent overview, such as Branch-and-Bound can then be used to solve the MINLP but depending on the size of the finite dimensional approximation these techniques may struggle. On the one hand, the discretization of the control might (especially for problems with a time-dependent control) result in a large amount of integer controls and thus an immense combinatorial complexity of the MINLP. On the other hand, the discretization of the PDE results in many equality constraints such that large-scale linear systems will occur whenever an NLP-relaxation of the MINLP has to be solved.

The contribution of this article to the field is to provide an alternative approach

*Department of Mathematics, Chemnitz University of Technology, Germany (dominik.garmatter@math.tu-chemnitz.de, martin.stoll@math.tu-chemnitz.de)

†Department of Mathematics, University of Bologna, Italy (margherita.porcelli@unibo.it)

‡Department of Mathematics "Tullio Levi-Civita", University of Padova, Italy (rinaldi@math.unipd.it)

for MIPDECO problems via penalty formulations. While penalty reformulations have been studied in the context of integer programming, see, e.g., [6, 10, 19, 26, 30], and penalty approaches have been developed, see, e.g., [5, 20, 22], there have been (to the knowledge of the authors) no contributions that explicitly deal with MIPDECO problems.

The general idea of penalty reformulations is to relax the integrality constraints of the problem and add a suitable penalty term to the objective function that penalizes controls that violate the previously present integrality constraints. A naive solution strategy could then be to iteratively solve the resulting penalty formulation while increasing the amount of penalization in each iteration and as a consequence one will end up with an integer solution at some point. The upside of such penalization strategies is that the combinatorial complexity of the integer constraints is eliminated from the problem formulation and the penalty term then ensures that the resulting solution satisfies the integer constraints. The downside is that penalty terms are usually concave such that one has to deal with non-convex NLPs with possibly an exponential amount of local minimizers.

To still provide qualitative solutions in the penalization context, the main contribution of this article is the development of a novel Improved Penalty Algorithm (IPA). Our algorithm is closely related to a family of existing Exact Penalty (EXP) algorithms analyzed both in the context of general constrained optimization [7, 25] and in the context of integer optimization [20]. Roughly speaking, a general EXP algorithmic framework, which is an iterative procedure, provides an automatic tool for when to increase penalization and when to aim for a better minimizer via a suitable global solver for the penalized subproblems. One then can show convergence towards a global minimizer of the original problem, see, e.g., [20, Corollary 1] for the analysis of the integer case.

A practical implementation of an EXP algorithm for a specific class of MIPDECO problems is described in the paper. The scheme embeds a suitably developed search approach, closely connected with Basin Hopping or Iterated Local Search methods, see, e.g., [13, 16], that combines a local optimization algorithm with a tailored perturbation strategy, and enables us to efficiently calculate an approximate solution of the penalty reformulation. As a proof of concept, the IPA is then applied to a stationary test problem and numerically compared to traditional penalty and rounding approaches as well as a Branch-and-Bound routine from CPLEX [1].

The remainder of this work is organized as follows: the model problem is presented and discretized in Section 2. Section 3 reviews the EXP algorithm and then develops the novel Improved Penalty Algorithm. Section 4 briefly collects the remaining algorithms for the numerical comparison carried out in Section 5.

2. Problem formulation. We begin with the description of the optimal control model problem in function spaces. After discretization we derive the reduced formulation as well as its continuous reformulation and conclude with remarks on extending the presented model problem to time-dependent problems.

2.1. Continuous optimal control problem. We begin with the description of the partial differential equation (PDE) in question in order to formulate the optimal control problem. Consider a bounded domain $\Omega \subset \mathbb{R}^2$, source functions $\phi_1, \dots, \phi_l \in C^\infty(\mathbb{R}^2)$ and based on these the PDE: for a given control $u = (u_1, \dots, u_l)^\top \in \mathbb{R}^l$ find

the state $y \in H_0^1(\Omega)$ solving

$$(1) \quad -\Delta y(x) = \sum_{i=1}^l u_i \phi_i(x), \quad x \in \Omega.$$

Existence and uniqueness of a solution $y \in H_0^1(\Omega)$ of (1) are secured via the Lax-Milgram theorem and we mention that this would already be fulfilled by source functions in $L^2(\Omega)$. We choose to model the sources ϕ_1, \dots, ϕ_l as Gaussian functions with centers $\tilde{x}_1, \dots, \tilde{x}_l \in \tilde{\Omega}$, and $\tilde{\Omega} \subset \Omega$, such that for $x \in \mathbb{R}^2$

$$(2) \quad \phi_i(x) := h e^{-\frac{\|x - \tilde{x}_i\|_2^2}{w}}, \quad i = 1, \dots, l,$$

with height $h > 0$ and width $w > 0$.

The optimal control problem in function spaces then reads: given a desired state $y_d \in L^2(\Omega)$, find a solution pair $(y, u) \in H_0^1(\Omega) \times \{0, 1\}^l$ of

$$(3) \quad \begin{aligned} \min_{y \in H_0^1(\Omega), u \in \{0, 1\}^l} \quad & \frac{1}{2} \|y - y_d\|_{L^2(\Omega)}^2, \\ \text{s.t.} \quad & (y, u) \text{ fulfill (1), and } \sum_{i=1}^l u_i \leq S \in \mathbb{N}. \end{aligned}$$

This problem can be interpreted as fitting a desired heating pattern y_d by activating up to S many heat sources. Since the amount of controls $u \in \{0, 1\}^l$ is finite and for each control there is a uniquely determined state y , problem (3) is in its essence a combinatorial problem such that existence of at least one global minimizer is guaranteed. We close this section with some remarks on the presented model problem.

Remark 2.1. (a) The choice of Gaussian source functions was motivated by porous-media flow applications to determine the number of boreholes [8, 23] and problem (3) with this choice of source functions is furthermore a model problem mentioned in [17, Section 19.3]. We will see throughout the remainder of this article that we do not rely on the chosen modelling of the control and that one could use for example piecewise constant sources as in [4] or a general distributed control as well.

(b) It is well-known that problems with general integer constraints can be reduced to problems with binary constraints, see, e.g., [11]. Furthermore, [19, Section 4] provides an alternative in the context of penalty approaches by directly penalizing general integer constraints. Extending the presented model problem from binary to general integer constraints and developing strategies to efficiently deal with these is an interesting aspect for future research.

2.2. Discretized problem and parabolic extension. Introducing a conforming mesh over Ω using N vertices, let $M \in \mathbb{R}^{N \times N}$ and $K \in \mathbb{R}^{N \times N}$ be the mass- and stiffness matrices of a corresponding finite element discretization of (1) using piecewise linear finite elements. Furthermore, the matrix $\Phi \in \mathbb{R}^{N \times l}$ contains the finite element coefficients of the Gaussian functions defined in (2) in its columns, i.e., each column contains the evaluation of the respective source function at the N vertices of the grid. With these matrices at hand, we formulate the *discretized optimal control problem*

$$(4) \quad \begin{aligned} \min_{y \in \mathbb{R}^N, u \in \{0, 1\}^l} \quad & \frac{1}{2} (y - y_d)^\top M (y - y_d), \\ \text{s.t.} \quad & Ky = M\Phi u, \quad \text{and} \quad \sum_{i=1}^l u_i \leq S \in \mathbb{N}. \end{aligned}$$

The inequality constraint in (4) is commonly referred to as a knapsack constraint. In (4) and for the remainder of this article, y denotes the vector of the finite element coefficients of the corresponding finite element approximation of (1) rather than the actual PDE-solution. The same holds true for the desired state y_d which from now on represents a finite element coefficient vector instead of an actual $L^2(\Omega)$ -function. Introducing the sets

$$(5) \quad W := \left\{ u \in \{0, 1\}^l \mid \sum_{i=1}^l u_i \leq S \right\} \quad \text{and} \quad X := \left\{ u \in [0, 1]^l \mid \sum_{i=1}^l u_i \leq S \right\}$$

as well as the matrices

$$G_1 := \Phi^\top M^\top K^{-\top} M K^{-1} M \Phi \in \mathbb{R}^{l \times l} \quad \text{and} \quad G_2 := M K^{-1} M \Phi \in \mathbb{R}^{N \times l},$$

we can formulate the *reduced optimal control problem*

$$(P) \quad \min_{u \in W} J(u) := \frac{1}{2} u^\top G_1 u - y_d^\top G_2 u + \frac{1}{2} y_d^\top M y_d$$

as well as its *continuous relaxation*

$$(P\text{cont}) \quad \min_{u \in X} J(u).$$

With M being a positive definite mass matrix, G_1 is positive definite as well and the objective function J of (P) is quadratic and convex. Additionally, X is a convex set such that (Pcont) is a convex optimization problem. We further note that problems (4) and (P) are equivalent in the sense that their minima coincide and we will consider the reduced formulation (P) for the remainder of this article.

The authors acknowledge that (P) might be tackled by existing methods, see, e.g., [4, 5, 22], and thus want to comment on the limitations of these approaches in a large-scale context.

1. In [4], a branch-and-cut algorithm is presented, where the computation of a cutting plane requires one linear PDE solution per dimension of the control space. Therefore, this approach can become excessively time-consuming for large l .
2. In [5], an EXP framework that embeds an iterative genetic algorithm is presented, where the amount of objective function evaluations per iteration usually scales quadratically with the problem dimension. In the PDE-constrained optimization context of (P) an evaluation of the objective function requires a possibly expensive PDE solution. Again, this can become too costly for large l .
3. In [22], a penalty-based approach combined with a smoothing method is considered to solve nonlinear and possibly non-convex optimization problems with binary variables. The main drawback in this case is: there is no theoretical guarantee that one converges towards the global minimum. Hence, the smoothing and penalty parameters need to be carefully initialized and handled during the optimization process in order to avoid getting stuck in bad local minima.

Although the presented model problem is neither of large scale in l nor in N , it can easily be scaled up by extending it towards a three-dimensional setup or parabolic PDEs as described in the upcoming remark.

Remark 2.2. Introducing the time interval $[0, T]$ with final time $T > 0$, the model problem (3) can be expanded to a time-dependent problem by introducing the parabolic PDE: for $\tilde{u} := (\tilde{u}_1(t), \dots, \tilde{u}_l(t))^\top \in \mathbb{R}^l \times (0, T)$, find $\tilde{y} \in L^2(0, T, H_0^1(\Omega))$ solving

$$(6) \quad \begin{aligned} \frac{\partial}{\partial t} \tilde{y}(t, x) - \Delta \tilde{y}(t, x) &= \sum_{i=1}^l \tilde{u}_i(t) \phi_i(x), \quad (t, x) \in (0, T) \times \Omega, \\ \tilde{y}(0, x) &= 0, \quad x \in \overline{\Omega}. \end{aligned}$$

A possible corresponding optimal control problem could then be: given a desired state $\tilde{y}_d \in L^2((0, T) \times \Omega)$, solve

$$(7) \quad \begin{aligned} \min_{\substack{\tilde{y} \in L^2(0, T, H_0^1(\Omega)) \\ \tilde{u} \in \{0, 1\}^l \times (0, T)}} \quad & \frac{1}{2} \|\tilde{y} - \tilde{y}_d\|_{L^2((0, T) \times \Omega)}^2, \\ \text{s.t.} \quad & (\tilde{y}, \tilde{u}) \text{ fulfill (6), and } \sum_{i=1}^l \tilde{u}_i(t) \leq S \in \mathbb{N}, \forall t \in (0, T). \end{aligned}$$

It is easy to see that after discretizing (7), the dimensions of both the PDE constraint and the control will scale with the number of time steps, so that the resulting discretized optimal control problem is of large scale both in l and N . We stress that the approach presented in the upcoming section aims at such large-scale problems and we plan to tackle such time-dependent problems in future work.

3. Improved Penalty Algorithm (IPA). This section contains the main contribution of this article, the development of our novel Improved Penalty Algorithm (IPA). We will first introduce a standard penalty reformulation of (P) that is equivalent to (P) in the sense that their global minima coincide followed by an Exact Penalty algorithm from [20]. Afterwards we will develop the IPA, which will be a modified version of the Exact Penalty algorithm in such a way that it can be applied to large-scale problems.

3.1. Penalty formulation and Exact Penalty (EXP) algorithm. Starting from the continuous relaxation (Pcont), we add the well-known penalty term

$$(8) \quad \frac{1}{\varepsilon} \sum_{i=1}^l u_i(1 - u_i)$$

to the objective function. Obviously, this concave penalty term penalizes a non-binary control, where $\varepsilon > 0$ controls the amount of penalization. This yields the following *penalty formulation*

$$(Ppen) \quad \min_{u \in X} J_p(u; \varepsilon) := J(u) + \frac{1}{\varepsilon} \sum_{i=1}^l u_i(1 - u_i).$$

PROPOSITION 3.1. *There exists an $\tilde{\varepsilon} > 0$ such that for all $\varepsilon \in (0, \tilde{\varepsilon}]$ problems (P) and (Ppen) have the same minimum points. Having the same minimum points here means that both problems (P) and (Ppen) have the same global minima (if there exist multiple). In this sense both problems (P) and (Ppen) are equivalent.*

Proof. Looking at problem (P) and the definition of the sets W and X in (5), we observe that $J \in C^1(\mathbb{R}^l)$ and that W and X are compact. Together with the results derived in [19, Section 3] all assumptions of [19, Theorem 2.1] are fulfilled such that the desired statement follows.

We mention that the equivalence result from Proposition 3.1 also holds for a variety of concave penalty terms, see, e.g., [19, (19)-(23)] or [26, (21)]. We chose the penalty term (8) in this article since it is a quadratic function and thus the combined objective function J_p remains quadratic.

Before we formulate the Exact Penalty algorithm, we introduce a rounding concept that respects the knapsack constraint in X and W and prove that it is the correct tool required for the algorithm design.

DEFINITION 3.2. *Let for $x \in X$ and $S \in \mathbb{N}$, with $S \leq l$, denote $x_S \in \mathbb{R}^S$ the S largest components of x . We then define the smart rounding $[x]_{SR} \in W$ of x as follows: round x_S component-wise to the closest integer and set the remaining components to 0.*

We illustrate the smart rounding by considering a simple example.

EXAMPLE 3.3. *Let $S = 2$ and $l = 3$ and let $[\cdot]$ denote the usual rounding to the closest integer. Then, for*

$$u_1 = (0.8, 0.7, 0.1)^\top \in X \quad \text{and} \quad u_2 = (0.63, 0.62, 0.61)^\top \in X$$

it is

$$\begin{aligned} [u_1]_{SR} &= (1, 1, 0)^\top \equiv [u_1] \in W, \quad \text{but} \\ [u_2]_{SR} &= (1, 1, 0)^\top \neq [u_2] = (1, 1, 1)^\top \notin W. \end{aligned}$$

Before proving the main property related to the smart rounding, we report the following definition.

DEFINITION 3.4. *We define the Chebyshev distance between a point $x \in \mathbb{R}^2$ and a set $C \subset \mathbb{R}^2$ as*

$$(9) \quad \text{dist}_\infty(x, C) = \min\{\|x - y\|_\infty \mid y \in C\}.$$

We now prove a property of the smart rounding that will be required for the convergence of the EXP algorithm.

PROPOSITION 3.5. *For $z \in W$, let $B(z)$ be the set*

$$B(z) := \{u \in \mathbb{R}^l \mid \|u - z\|_\infty \leq \rho\}$$

where $\rho > 0$ is chosen such that

$$B(z_a) \cap B(z_b) = \emptyset, \quad \text{for all } z_a, z_b \in W \text{ with } z_a \neq z_b.$$

Given a point $\bar{u} \in X$, then the point $\bar{z} := [\bar{u}]_{SR} \in W$ minimizes the Chebyshev distance between \bar{u} and the sets $B(z)$ with $z \in W$, that is

$$\bar{z} \in \arg \min_{z \in W} \text{dist}_\infty(\bar{u}, B(z)).$$

Proof. If there exists a $z \in W$ such that $\bar{u} \in B(z)$, then it has to be $z \equiv \bar{z} = [\bar{u}]_{SR}$. In this trivial case, we have $\text{dist}_\infty(\bar{u}, B(\bar{z})) = 0$ and the result follows.

Therefore, we assume in the following that $\bar{u} \notin B(z)$ for all $z \in W$. By contradiction, there then exists a point $\hat{z} \in W$ satisfying

$$(10) \quad \text{dist}_\infty(\bar{u}, B(\hat{z})) < \text{dist}_\infty(\bar{u}, B(\bar{z})).$$

We can hence find two points $\hat{p} \in B(\hat{z})$ and $\bar{p} \in B(\bar{z})$ satisfying

$$(11) \quad \|\hat{p} - \bar{u}\|_\infty = \text{dist}_\infty(\bar{u}, B(\hat{z})) \quad \text{and} \quad \|\bar{p} - \bar{u}\|_\infty = \text{dist}_\infty(\bar{u}, B(\bar{z})).$$

It is easy to see that

$$(12) \quad \|\hat{p} - \hat{z}\|_\infty = \|\bar{p} - \bar{z}\|_\infty = \rho$$

and from (11) we further obtain

$$(13) \quad \|\bar{u} - \hat{z}\|_\infty = \|\bar{u} - \hat{p}\|_\infty + \|\hat{p} - \hat{z}\|_\infty \quad \text{and} \quad \|\bar{u} - \bar{z}\|_\infty = \|\bar{u} - \bar{p}\|_\infty + \|\bar{p} - \bar{z}\|_\infty.$$

So far, we can conclude from equations (10)-(13) that

$$(14) \quad \|\bar{u} - \bar{z}\|_\infty - \|\bar{u} - \hat{z}\|_\infty = \|\bar{u} - \bar{p}\|_\infty + \underbrace{\|\hat{p} - \bar{z}\|_\infty}_{=\rho} - \|\bar{u} - \hat{p}\|_\infty - \underbrace{\|\hat{p} - \hat{z}\|_\infty}_{=\rho} > 0.$$

Now, taking into account the fact that $\bar{z} = [\bar{u}]_{SR} \neq \hat{z}$, we need to have at least one component $i \in I = \{1, \dots, l\}$ such that $\bar{z}_i \neq \hat{z}_i$. Let us now define the set

$$I_L := \{i \in I \mid \bar{u}_i \geq 0.5\}.$$

If $|I_L| < S$, we have $[\bar{u}]_{SR} = [\bar{u}]$ and it is easy to see

$$\|\bar{u} - \bar{z}\|_\infty \leq \|\bar{u} - \hat{z}\|_\infty,$$

thus getting a contradiction to (14).

Therefore, we assume that $|I_L| \geq S$ in the following and define the set I_S , with $|I_S| = S$, so that $\bar{u}_i > \bar{u}_j$ for all $i \in I_S$ and $j \in I_L \setminus I_S$, i.e., the index set of the S largest components of \bar{u} . By the definition of the smart rounding, it is then obvious that $\bar{z}_i = 1$ for $i \in I_S$ and $\bar{z}_i = 0$ for $i \in I \setminus I_S$.

Now, any $\tilde{z} \in W$ can be obtained from \bar{z} by considering any combination of the following operations:

1. $\bar{z}_i = 1 \rightarrow \tilde{z}_i = 0$ for one $i \in I_S$;
2. $\bar{z}_i = 1 \rightarrow \tilde{z}_i = 0$ for one $i \in I_S$ and $\tilde{z}_j = 1$ for one $j \in I \setminus I_L$;
3. $\bar{z}_i = 1 \rightarrow \tilde{z}_i = 0$ for one $i \in I_S$ and $\tilde{z}_j = 1$ for one $j \in I_L \setminus I_S$.

Since $\bar{u}_i \geq 0.5$ for all $i \in I_S$ the first part of any of the mentioned operations results in

$$|\bar{u}_i - \bar{z}_i| \leq |\bar{u}_i - \tilde{z}_i|.$$

In the second operation $j \in I \setminus I_L$ implies that $\bar{u}_j < 0.5$ and $\bar{z}_j = 0$ and we obtain

$$|\bar{u}_j - \bar{z}_j| \leq |\bar{u}_j - \tilde{z}_j|.$$

In the third operation $j \in I_L \setminus I_S$ implies that $\bar{u}_j \geq 0.5$ but $\bar{z}_j = 0$ such that

$$|\bar{u}_j - \bar{z}_j| \geq |\bar{u}_j - \tilde{z}_j|.$$

Taking the whole third operation into account and remembering that $i \in I_S$ as well as the definition of the smart rounding, we can see that

$$\max\{|\bar{u}_j - \bar{z}_j|, |\bar{u}_i - \bar{z}_i|\} \leq \max\{|\bar{u}_j - \tilde{z}_j|, |\bar{u}_i - \tilde{z}_i|\}.$$

Forming any $\tilde{z} \in W$ from \bar{z} via these operations thus implies that

$$\|\bar{u} - \bar{z}\|_\infty \leq \|\bar{u} - \tilde{z}\|_\infty$$

and as especially $\hat{z} \in W$ can be obtained from \bar{z} , we have

$$\|\bar{u} - \bar{z}\|_\infty \leq \|\bar{u} - \hat{z}\|_\infty,$$

which is a contradiction to (14). Hence, we get that

$$\text{dist}_\infty(\bar{u}, B(\hat{z})) \geq \text{dist}_\infty(\bar{u}, B(\bar{z})),$$

which concludes the proof.

With this result at hand, we state in Algorithm 1 the adaptation of the EXP algorithm from [20, Section 4] to our model problem (Ppen).

Algorithm 1 EXP($\varepsilon^0 > 0, \delta^0 > 0, \sigma \in (0, 1)$)

1: $n = 0, \varepsilon^n = \varepsilon^0, \delta^n = \delta^0$

2: **Step 1.** Compute $u^n \in X$ such that

$$(15) \quad J_p(u^n; \varepsilon^n) \leq J_p(u; \varepsilon^n) + \delta^n$$

for all $u \in X$.

3: **Step 2.**

4: **if** $u^n \notin W$ **and** $J_p(u^n; \varepsilon^n) - J_p([u^n]_{SR}; \varepsilon^n) \leq \varepsilon^n \|u^n - [u^n]_{SR}\|_2$ **then**

5: $\varepsilon^{n+1} = \sigma\varepsilon^n, \delta^{n+1} = \delta^n$

6: **else**

7: $\varepsilon^{n+1} = \varepsilon^n, \delta^{n+1} = \sigma\delta^n$

8: **end if**

9: **Step 3.** Set $n = n + 1$ and go to Step 1.

Algorithm 1 assumes that in Step 1 a δ -global optimizer, i.e., an iterate $u^n \in X$ that fulfills (15), can be found, for example via a global optimization method, see, e.g., [18] for an overview of existing methods. Step 2 of the algorithm then provides a tool to decide when to increase penalization and when to seek for a better global minimizer. The main convergence property of Algorithm 1 is reported in the upcoming Proposition 3.6 and shows that Algorithm 1 extends global optimization methods for continuous problems to integer problems.

PROPOSITION 3.6. *Every accumulation point \bar{u} of a sequence of iterates $\{u^n\}_{n \in \mathbb{N}}$ of Algorithm 1 is a global minimizer of (P).*

Proof. Using Proposition 3.5 the statement follows from [20, Corollary 1].

Before we develop our novel algorithm in the upcoming section, we want to comment on the second condition in line 4 of Algorithm 1: this condition is based on [20, (3)], a Hoelder-condition for the unpenalized objective function. Since our objective function J is quadratic, it is Hoelder-continuous with Hoelder-exponent equal to 1. Furthermore, β (corresponding to the Hoelder-constant), that appears in the original formulation of the algorithm in [20, Section 4], can for simplicity be set to 1 since this only influences the convergence speed of the algorithm.

3.2. Development of the Improved Penalty Algorithm (IPA). Based on the EXP algorithm from the previous section, we now want to develop our novel algorithm. In the practical implementation, we do not require a δ -global optimizer in Step 1 of Algorithm 1 but instead want to compute an iterate $u^n \in X$ that reduces the

objective function such that $J_p(u^n; \varepsilon^n) < J_p(u^{n-1}; \varepsilon^n)$. Do note that this corresponds to Step 1 of Algorithm 1 but with an unknown rule of reducing δ .

Algorithm 1 could be overall terminated as soon as δ is smaller than some tolerance. Since there is no explicit δ in our approach anymore, we terminate our algorithm as soon as we are unable to find a new iterate that reduces the objective function.

Both these adjustments are collected in the Sub-Algorithm 2.a where we aim at improving the current iterate by perturbing it and utilizing this perturbation as initial guess for the local solver. This strategy is closely connected with classic Basin Hopping or Iterated Local Search strategies, see, e.g., [13, 16], for global optimization problems. The sub-algorithm is then terminated after a certain amount of these perturbation cycles and this bears the information that no better iterate could be found. Gathering these thoughts results in the *Improved Penalty Algorithm (IPA)*, i.e., Algorithm 2 reported below.

Algorithm 2 Improved Penalty Algorithm ($u^0, \varepsilon^0 > 0, \sigma \in (0, 1)$)

```

1:  $n = 0, u^n = u^0, \varepsilon^n = \varepsilon^0$ 
2: Step 1. Call Algorithm 2.a( $u^n, \varepsilon^n$ ) to generate a new iterate  $u^{n+1}$ .
3: Step 2.
4: if  $u^{n+1} \notin W$  and  $J_p(u^{n+1}; \varepsilon^n) - J_p([u^{n+1}]_{SR}; \varepsilon^n) \leq \varepsilon^n \|u^{n+1} - [u^{n+1}]_{SR}\|_2$  then
5:    $\varepsilon^{n+1} = \sigma \varepsilon^n$ 
6: else
7:    $\varepsilon^{n+1} = \varepsilon^n$ 
8: end if
9: Step 3.
10: if  $u^n \equiv u^{n+1}$  then
11:   return  $[u^{n+1}]_{SR}$ 
12: else
13:   Set  $n = n + 1$  and go to Step 1.
14: end if

```

Algorithm 2.a Reduction via Perturbation(u, ε)

```

1:  $u^{init} = u$ 
2: for  $j = 1, \dots, p_{\max}$  do
3:   Use a local solver to determine a solution  $u^{loc}$  of (Ppen) for  $\varepsilon$  using  $u^{init}$  as
   initial guess.
4:   if  $J_p(u^{loc}; \varepsilon) < J_p(u; \varepsilon)$  then
5:     return  $u^{loc}$ 
6:   else
7:     Generate a point  $u^{pert} = Perturbation(u^{loc})$  and set  $u^{init} = u^{pert}$ .
8:   end if
9: end for
10: return  $u$ 

```

Do note that if the for-loop in Algorithm 2.a does finish (and thus no better iterate was found after p_{\max} perturbations), the algorithm terminates with u which was the input iterate. In that case it is $u^{n+1} \equiv u^n$ and the overall Algorithm 2 then terminates. Therefore, the perturbation strategy in Algorithm 2.a together with the choice of p_{\max} determine at what point no reduction in the objective function can be

found anymore. Algorithm 2.a does not specify a perturbation strategy at line 7 and one can develop a strategy that does fit the problem in question. We will present our strategy in the numerical Section 5.2.

While ε is decreased during Algorithm 2 (and thus the amount of penalization is increased), the concave penalty term (8) introduces local minima to $J_p(u; \varepsilon)$ near the integer points of X which, as ε is decreased, move towards the integer points. Due to this behavior, the condition $J_p(u^{loc}; \varepsilon^n) < J_p(u; \varepsilon^n)$ in line 4 of Algorithm 2.a is always fulfilled as long as $\varepsilon^n < \varepsilon^{n-1}$ holds in Algorithm 2. By this, we expect Algorithm 2 to have a two-phase behavior: in the first phase, the penalization is increased until a feasible iterate $u^{n+1} \in W$ is found. In the second phase, Algorithm 2.a then tries to improve the current iterate by perturbing it and restarting the local solver with this perturbed iterate. This way, one wants to escape bad basins of attraction of J_p and then move towards better local minima and eventually the global one.

Depending on the perturbation strategy and for large enough p_{\max} , the search strategy described in Algorithm 2.a would again find a δ -global optimizer (for an unknown δ) and Algorithm 2 would reproduce Algorithm 1. The central difference now is that Algorithm 2.a only requires a local solver. Therefore, Algorithm 2 should be applicable to large-scale problems: the combinatorial complexity induced by a large control is taken care of via the penalty term as well as the framework of the EXP algorithm, and a large N induced by for example a parabolic PDE can be handled via a sophisticated local solver.

Finally, we want to mention that a new iterate u^{n+1} found by Algorithm 2.a is always feasible so that $u^{n+1} \in X$. Thus, the criterion $u^{n+1} \notin W$ in line 4 of Algorithm 2 can, in an actual implementation, be replaced by

$$\|u^{n+1} - [u^{n+1}]_{SR}\|_{\infty} > \epsilon_{feas}$$

with some feasibility tolerance ϵ_{feas} .

4. Other algorithms included in the numerical comparison. In this section, we shortly present three solution strategies for (P) that will then be compared to Algorithm 2 via numerical experiments in Section 5. The strategies presented in this section include: a naive penalty algorithm, a Branch-and-Bound routine and a simple rounding strategy.

4.1. A simple penalty algorithm. Starting with the penalty formulation (Ppen), we use the following naive iterative approach: given a feasible initial guess $u^0 \in X$, an initial penalty parameter $\varepsilon^0 > 0$ and $n = 0$

1. use a local solver to determine a solution $u^{n+1} \in X$ of (Ppen) for ε^n using u^n as initial guess,
2. stop if $u^{n+1} \in W$, else set $\varepsilon^{n+1} = \sigma\varepsilon^n$ ($\sigma \in (0, 1)$), $n = n + 1$ and go to the first step.

As mentioned in the previous section, instead of checking for $u^{n+1} \in W$ one can use the criterion $\|u^{n+1} - [u^{n+1}]_{SR}\|_{\infty} < \epsilon_{feas}$ with some feasibility tolerance ϵ_{feas} . Putting these thoughts into an algorithm, we end up with the *Penalty Algorithm*, i.e., Algorithm 3.

Algorithm 3 is a simplification of Algorithm 2 in several ways. The penalty parameter is reduced in every iteration, a new iterate u^{n+1} generated by the local solver is always accepted as such, and the algorithm terminates as soon as an iterate $u^{n+1} \in W$ is found. By this, there is no theoretical framework that might support the algorithm anymore and one has to hope that the iterates approach the global minimizer of (P), or at least a good local minimizer.

Algorithm 3 Penalty($u^0, \varepsilon^0, \sigma \in (0, 1)$)

-
- 1: $n = 0, u^n = u^0, \varepsilon^n = \varepsilon^0$
 - 2: **repeat**
 - 3: Use a local solver to determine a solution u^{n+1} of (Ppen) for ε^n using u^n as initial guess.
 - 4: $\varepsilon^{n+1} = \sigma\varepsilon^n$
 - 5: $n = n + 1$
 - 6: **until** $\|u^n - [u^n]_{SR}\|_\infty < \epsilon_{feas}$
 - 7: **return** $[u^n]_{SR}$
-

We can also interpret Algorithm 3 as a more sophisticated rounding strategy: starting from the initial guess u^0 , by slowly decreasing ε (and thus increasing penalization of a non-binary control), the components of the control are then component-wise slowly driven towards either 0 or 1.

Finally, do note that the condition $\|u^n - [u^n]_{SR}\|_\infty < \epsilon_{feas}$ in line 6 of Algorithm 3 only detects if we consider the current iterate to be close enough to an integer. The output of the algorithm is then $[u^n]_{SR} \in W$.

4.2. Rounding and Branch-and-Bound. To complete this algorithmic overview, we present a simple rounding strategy and shortly comment on the Branch-and-Bound routine that will be used in the numerical discussion in Section 5. We chose to include a rounding strategy in the numerical comparison, since an algorithm should at least be able to beat simple rounding strategies to be considered viable.

We neither go into details of the Branch-and-Bound framework here nor present an actual Branch-and-Bound routine. We rather refer the reader to [3] for an elaborate overview of the topic. For the numerical comparison that will be carried out in Section 5, we will utilize `cplexmiqp`, the Branch-and-Bound routine of CPLEX [1] for quadratic mixed integer problems, to solve (P). Do note that this algorithm incorporates many algorithmic features lately developed to improve Branch-and-Bound performance.

As the rounding strategy, we simply determine the solution of the continuous relaxation (Pcont), denoted u^{cont} here, and output $[u^{cont}]_{SR}$, i.e., apply the smart rounding from Definition 3.2 to u^{cont} .

5. Numerical experiments and discussion. We want to compare Algorithm 2/2.a to the various solution strategies presented in Section 4, i.e., Algorithm 3, the simple rounding strategy and CPLEXs Branch-and-Bound routine `cplexmiqp`. To this end, we first formulate the general setting in which the experiments will take place followed by algorithmic specifications including a discussion on our implementation of Algorithm 2, and then conduct several experiments.

5.1. Setting and algorithmic specifications. We choose $\Omega := [0, 1]^2$ as our computational domain for the numerical experiments. Regarding the Gaussian sources defined in (2), we choose $l = 100$ sources with centers $\tilde{x}_1, \dots, \tilde{x}_l$ being arranged in a uniform 10×10 grid over $\tilde{\Omega} := [0.1, 0.9]^2 \subset \Omega$. The height of the sources is $h = 100$ and the width w is chosen such that every source takes 5% of its center-value at a neighboring center. We mention that this choice of height and width is motivated by [28, Section 4.2]. Piecewise linear finite elements are used for the discretization of (1) and the grid consists of 5000 regular finite elements resulting in $N = 51^2$ vertices.

Whenever a local solver is required, i.e, in Algorithms 2.a and 3 as well as for

the solution of the continuous relaxation for the rounding strategy, we use Matlab's `fmincon` [2] with its interior point solver. The choice of this solver is motivated by its good performance during our tests but we do note that any other solver being able to successfully handle optimization problems with a quadratic, non-convex objective function and a convex feasible region could be equally employed at this stage. Furthermore, the solution of (Pcont) obtained this way is then also used as the initial guess of Algorithms 2 and 3. Do note that this is no necessity since (Ppen) for large enough ϵ^0 is then still a convex problem in the first iteration of these algorithms so that any initial guess would be sufficient. Specifically, we use $\epsilon^0 = 10^6$ for both algorithms as well as $\sigma = 0.9$ for Algorithm 3 and $\sigma = 0.5$ for Algorithm 2. The more conservative value of σ for Algorithm 3 is necessary here, since with σ being much closer to 0 one would risk increasing the amount of penalization too fast and thus settling for an unsatisfactory local minimum. Finally, we used the feasibility tolerance $\epsilon_{feas} = 0.01$ in Algorithm 3 and, as discussed at the end of Section 3.2, in line 4 of Algorithm 2.

The remaining details of our implementation of Algorithm 2, i.e., the perturbation strategy used in Algorithm 2.a and the termination of the algorithm, will be discussed in the upcoming Section 5.2.

Regarding `cplexmiqp`, we use default options (such that the algorithm determines an initial guess on its own) except that we set a time limit of 3600 seconds and a memory limit of 16000 megabytes for the search tree.

Remark 5.1. The authors want to emphasize that `cplexmiqp` typically performs better for the full formulation (4). For a consistent comparison we here nevertheless apply `cplexmiqp` to the reduced problem. Future work will compare `cplexmiqp` to a tailored expansion of our scheme for the full formulation as this will be needed for three-dimensional and time-dependent PDEs.

All experiments were conducted on a PC with 32 GB RAM and a QUAD-Core-Processor INTEL-Core-I7-4770 (4x 3400MHz, 8 MB Cache) utilizing Matlab 2019a via which CPLEX 12.9.0 was accessed.

5.2. Implementation details of the IPA. We start with the presentation of our perturbation strategy used in Algorithm 2.a. The details are described in Algorithm 2.b.

Algorithm 2.b Perturbation(u)

- 1: $u^{pert} := u$
 - 2: Find I_S the set containing the indices of the S largest entries of u .
 - 3: **for** $j = 1, \dots, \theta$ **do**
 - 4: Randomly select $\hat{i} \in I_S$.
 - 5: Define I_{adj} the set of indices corresponding to sources *adjacent* to $\tilde{x}_{\hat{i}}$.
 - 6: Randomly select $\hat{i}_{adj} \in I_{adj}$.
 - 7: Set $(u^{pert})_{\hat{i}}$ to a randomly chosen value smaller than $\frac{1}{2}$.
 - 8: Set $(u^{pert})_{\hat{i}_{adj}}$ to a randomly chosen value larger than $\frac{1}{2}$.
 - 9: Remove \hat{i} from I_S .
 - 10: **end for**
 - 11: **return** u^{pert}
-

When Algorithm 2.b is called by Algorithm 2.a inside Algorithm 2, u is equal to the current iterate u^n . The algorithm then essentially performs $\theta \in \mathbb{N}$ *flips* to the current iterate, where a flip is one iteration of the for-loop of Algorithm 2.b, i.e.,

a large value of u^n is set to a small value and an entry of u^n corresponding to a source that is *adjacent* to the source corresponding to the large value is set to a large value. By this strategy the resulting perturbation u^{pert} should lie outside the current basin of attraction and therefore be an interesting initial guess for the local solver in Algorithm 2.a. It remains to explain what we mean by *adjacent* in the above context

Based on our choice of using a uniform 10×10 grid of sources, we let $p = 10$ and define I_{adj} the index set of sources adjacent to \tilde{x}_i in the case when \tilde{x}_i is an interior source as

$$(16) \quad \{\hat{i} - 1, \hat{i} + 1, \hat{i} - p - 1, \hat{i} - p, \hat{i} - p + 1, \hat{i} + p - 1, \hat{i} + p, \hat{i} + p + 1\}.$$

Since \tilde{x}_i is assumed to correspond to an interior source this set corresponds to the indices of all sources that are direct neighbors of \tilde{x}_i in the $p \times p$ grid of sources. Obviously this set has to be adjusted if \tilde{x}_i is on the boundary of the source grid.

Although the perturbation strategy presented so far depends on the uniform grid of source centers in order to determine the index set I_{adj} , the underlying concept of this *flipping* does not depend on the chosen modelling. The large component $(u^{pert})_{\hat{i}}$ of the control can often be associated to a spatial counterpart denoted, for the purpose of clarity, as x_i here. In our case this is $x_i = \tilde{x}_i$, the center of the Gaussian source function. If the control would be modeled via for example piecewise constant functions $\{\chi_i(x)\}_{i=1}^l$ as in [4], x_i could be the center of the patch of the domain that corresponds to $\chi_i(x)$. If the control would be distributed, x_i would be the vertex of the grid that corresponds to u_i . Finding the set of *adjacent indices* in line 5 of Algorithm 2.b then translates to selecting all indices that correspond to spatial counterparts \bar{x} with $\|x_i - \bar{x}\| \leq r$, where the radius $r > 0$ controls the degree of *adjacency*. For example, the set of indices in (16) could be generated with the radius $r = \frac{\sqrt{2}}{p+1}$.

With this interpretation, as long as the control can be associated to spatial counterparts of the domain Ω , the presented perturbation strategy can easily be applied to different kinds of controls and models. Do also note that the choice of $\Omega = [0, 1]^2$ is not restrictive here and the approach can easily be extended to other domains.

Finally, we found it effective in our experiments to set $(u^{pert})_{\hat{i}}$ to a random value in $[0.1, 0.2]$ and to set $(u^{pert})_{\hat{i}_{adj}}$ to a random value in $[0.6, 0.8]$ during Algorithm 2.b. The underlying idea is to not choose values that are too close to 0 or 1. By this, u^{pert} is then an initial guess for the local solver in Algorithm 2.a that lies outside the current basin of attraction and is also not too close to other local minimizers (at this stage of the IPA there are local minimizers nearby all integer points).

In the remainder of this section, we want to discuss the termination of Algorithm 2.a and thus Algorithm 2.

The criterion $J_p(u^{loc}; \varepsilon^n) < J_p(u^n; \varepsilon^n)$ in Algorithm 2.a (as it is called inside Algorithm 2 with $u = u^n$ and $\varepsilon = \varepsilon^n$) can be numerically challenging in an actual implementation. Although the criterion should be fulfilled when it was $\varepsilon^n < \varepsilon^{n-1}$ in Algorithm 2 as mentioned in Section 3.2, this might not be the case numerically since any local solver used in Algorithm 2.a only computes u^{loc} up to some internal tolerance. Furthermore, if u^n is close to an integer already, we do not want to accidentally fulfill $J_p(u^{loc}; \varepsilon^n) < J_p(u^n; \varepsilon^n)$ due to numerical effects although $[u^{loc}] \equiv [u^n]$ such that no progress towards a better integer solution would be made. To cover both of these cases in our implementation, we replaced the criterion by the following two criteria and thus return u^{loc} in Algorithm 2.a if one of these is fulfilled.

1. If $u^{loc} \notin W$, i.e., $\|u^{loc} - [u^{loc}]_{SR}\|_{\infty} > \epsilon_{feas}$, and it is either $J_p(u^{loc}; \varepsilon^n) < J_p(u^n; \varepsilon^n)$ or $\frac{|J_p(u^{loc}; \varepsilon^n) - J_p(u^n; \varepsilon^n)|}{|J_p(u^{loc}; \varepsilon^n)|} < \epsilon_{red}$.

2. If $u^{loc} \in W$, i.e., $\|u^{loc} - [u^{loc}]_{SR}\|_\infty \leq \epsilon_{feas}$, and if additionally
- $$\frac{J_p(u^{loc}; \varepsilon^n) - J_p(u^n; \varepsilon^n)}{J_p(u^{loc}; \varepsilon^n)} < -\epsilon_{red}.$$

The first criterion targets the case when $J_p(u^{loc}; \varepsilon^n) \not\prec J_p(u^n; \varepsilon^n)$ numerically (although it was $\varepsilon^n < \varepsilon^{n-1}$ in Algorithm 2) and thus also accepts infeasible iterates with a small relative error towards the previous iterate. We mention that this usually happens during the first phase of the IPA where the amount of penalization is increased (due to $\varepsilon^{n+1} = \sigma \varepsilon^n$) and is not yet large enough for the local solver to produce near integer solutions fulfilling $\|u^{loc} - [u^{loc}]_{SR}\|_\infty \leq \epsilon_{feas}$. As a result it is not necessary to search for better solutions via the perturbation strategy such that this criterion tries to prevent non-productive iterations in Algorithm 2.a. If a feasible iterate was found, the second criterion wants to achieve a reduction in the objective function by at least $100 \cdot \epsilon_{red}\%$, with a possible reduction tolerance of $\epsilon_{red} = 0.01$. It thus enforces progress towards a better integer solution and should prevent the algorithm from getting stuck in an unsatisfactory local minimum. As in Algorithm 3, we use the feasibility tolerance $\epsilon_{feas} = 0.01$.

Finally we mention that choosing ϵ_{red} is a difficult task and therefore Algorithm 2.a still might terminate after p_{\max} steps with $u^{n+1} \equiv u^n$ and $u^{n+1} \notin W$, which means that Algorithm 2 is still in the phase where penalization needs to be increased. Surely, we do not want to terminate the whole algorithm in this case. Luckily, one can detect this behavior as ε must have been reduced in the previous iteration of Algorithm 2 and we simply continue Algorithm 2 if this occurred.

5.3. Experiments. We will conduct three different experiments. In the first experiment we will investigate the performance of the Improved Penalty Algorithm (IPA), i.e., Algorithm 2, with respect to $p_{\max} \in \mathbb{N}$ and $\theta \in \mathbb{N}$, i.e., how these choices in Algorithms 2.a and 2.b affect the solution quality and solution time of the algorithm. In the second experiment we will test the robustness of the stochastic component of Algorithm 2, i.e., how the random choices in Algorithm 2.b affect the solution time and quality of the overall algorithm. In the third experiment we compare Algorithm 2 to the various solution strategies presented in Section 4.

5.3.1. First experiment. For the first experiment we generate a test set of desired states, which contains 100 different desired states for each value of $S \in \{3, 6, 10, 15, 20\}$. Each desired state y_d in this test set is a solution of (the discretized version of) (1) with S active sources in the right-hand side and the centers of these sources are randomly distributed over $\tilde{\Omega} = [0.1, 0.9]^2$. The height and width of these sources coincide with the values that were used for the source-grid in Section 5.1. Surely, the combinatorial complexity of the optimization problem corresponding to such a desired state increases drastically for larger values of S and this will be a good challenge for `cplexmiqp` as well as the stochastic component of Algorithm 2 in the last experiment, where we will use a test set generated as described above but different from the one used for this experiment. To further illustrate the optimization problem here, Figure 1 exemplarily shows two desired states, one for $S = 3$ and one for $S = 20$, where the white stars depict the centers of the 100 Gaussian sources of the source grid and the red stars depict the centers of the S active sources in y_d .

In order to investigate the IPA with respect to $p_{\max} \in \mathbb{N}$, the amount of perturbation cycles in Algorithm 2.a, and $\theta \in \mathbb{N}$, the amount of flips per perturbation in Algorithm 2.b, we solve the created test set with the IPA using the following nine different Variations.

- Variations 1 – 3: for $S \in \{3, 6, 10, 15, 20\}$ we always choose $\theta \in \{2, 3, 4, 5, 6\}$

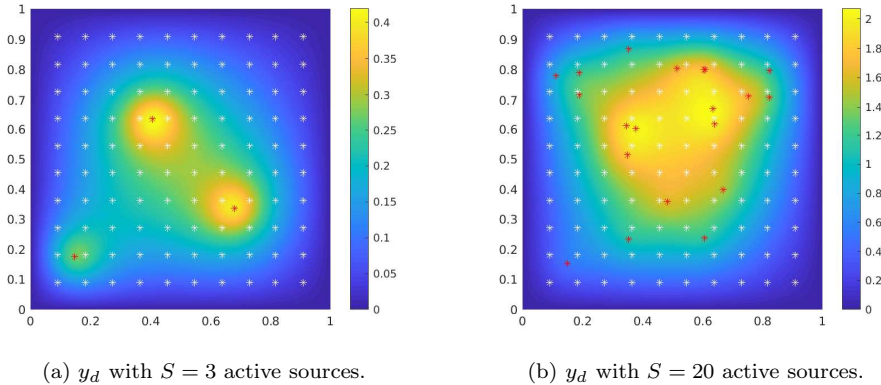


Fig. 1: Exemplary desired states including the centers of the source grid (white stars) and the centers of the active sources of the respective desired state (red stars).

and p_{\max} varies as $p_{\max} \in \{100, 200, 300\}$.

- Variations 4 – 6: for $S \in \{3, 6, 10, 15, 20\}$ we always choose $\theta \in \{3, 4, 5, 6, 7\}$ and p_{\max} varies as $p_{\max} \in \{100, 200, 300\}$.
- Variation 7 – 9: it is always $\theta = 3$ and p_{\max} varies as $p_{\max} \in \{100, 200, 300\}$.

After solving the test set with these 9 variations of the IPA, we compare the results with respect to solution time and quality. For the solution time, we report 't_av' the average solution time and for the solution quality, we choose the following two criteria.

- 'min_count': in each of the 100 runs for a value of S , it is noted which algorithm (here the 9 variations of the IPA) achieved the smallest objective function value and this algorithm is then awarded a 'min_count'-score. Surely, multiple algorithms can be awarded a score in the same run, e.g., when multiple algorithms find the global minimum.
- 'rel_err_av': the average relative error. In each of the 100 runs for a value of S , we also store for each algorithm (again the 9 variations of the IPA in this first experiment) the relative error between the objective function value achieved by that algorithm and the smallest objective function value in that run (the one that was awarded a 'min_count'-score). As the relative error is 0 for an algorithm if the algorithm was awarded a 'min_count'-score, only runs that produced a non-zero relative error are taken into account when computing the average relative error for an algorithm.

We chose to measure the quality of the algorithms via the described two quantities, since as the centers of the desired states in the test set are randomly distributed over Ω , the global minimum of the corresponding optimization problem is not known analytically. Therefore, the 'min_count'-value simply tells us how often an algorithm performed best compared to the other algorithms. The average relative error is an additional useful measure of quality since it tells us how good an algorithm performed (in average) in the cases, where the algorithm was not awarded a 'min_count'-score, i.e., how large the average error of this algorithm is compared to the best possible solutions among the tested algorithms. As an additional interpretation we note that in the third experiment the IPA will be compared to amongst others the Branch-and-Bound routine `cplexmiqp`. Since `cplexmiqp` does find a global minimizer whenever it

finishes (do note the restrictions imposed on the solver noted in Section 5.1) and if it does so in all 100 instances for a value of S in a test set, the 'min_count'-value of other algorithms then tells us how often that algorithm also found the global minimum.

The results of this first experiment can be seen in Figure 2, where the color of the plot indicates the results for the different values of S , i.e., $S = 3$ (blue circles), $S = 6$ (green crosses), $S = 10$ (red crosses), $S = 15$ (turquoise stars) and $S = 20$ (pink boxes), and the x-axis encodes the different variations of the IPA.

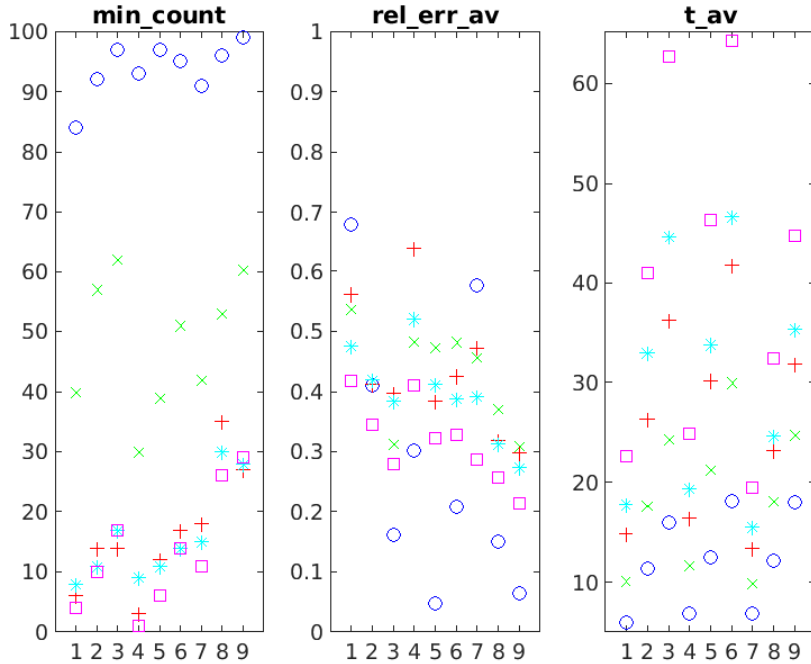


Fig. 2: Results of the first experiment. Data for $S = 3$ (blue circles), $S = 6$ (green crosses), $S = 10$ (red crosses), $S = 15$ (turquoise stars) and $S = 20$ (pink boxes) is plotted over the nine different variations.

Before we discuss the results of this first experiment in detail and in order to better understand the displayed data, we have a look at Figure 2.a, which contains only the 'min_count' data of the first experiment for $S = 6$ over the nine different variations.

As mentioned the x-axis represents the nine different variations of the first experiment. As an example, the left-most data point in Figure 2.a means: from the 100 different desired states for $S = 6$ contained in the test set of the first experiment, the IPA with variation 1 described above, i.e., for $S \in \{3, 6, 10, 15, 20\}$ we always choose $\theta \in \{2, 3, 4, 5, 6\}$ (and as $S = 6$ in Figure 2.a we have $\theta = 3$) and $p_{\max} = 100$, got a 'min_count'-score of 40. Remembering the definition of the 'min_count', this means that compared to the other eight variations of the IPA in the first experiment, variation 1 found the smallest objective function value available amongst these nine variations in 40 out of the 100 runs. In the same way, i.e., the x-axis encoding the

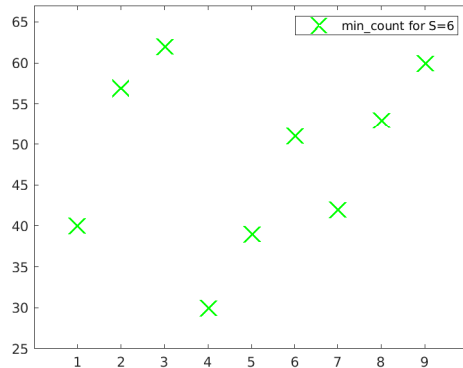


Fig. 2.a: Results of the first experiment: only the 'min_count' data for $S = 6$ is plotted over the nine different variations.

variation of the IPA and the color encoding the part of the test set corresponding to a value of S , the data points in the second and third picture of Figure 2 have to be understood.

Having understood the displayed data, we move on to the discussion of the results of the first experiment displayed in Figure 2. The main observation from this experiment is that variation 9 ($\theta = 3$, $p_{\max} = 300$) performs best with respect to solution quality. It has the highest 'min_count'-score for $S = 3$ and $S = 20$ and the second highest score for the remaining values of S , where only for $S = 10$ variation 8 has a significantly higher value. This observation is further enhanced as variation 9 has the smallest relative average error for all values of S such that it is superior to variation 8. Having a look at the average solution time, we can observe that increasing p_{\max} has much more influence on the solution time than increasing θ . This is expected as an increased p_{\max} directly results in more calls of the local solver in Algorithm 2.a as the IPA can only terminate when it was confirmed in Algorithm 2.a that no better iterate was found after p_{\max} iterations. Comparing the average solution times for variations 8 and 9 we surely see that variation 9 needs more time but taking the solution quality into account this additional time seems well invested. Furthermore, we conclude that choosing θ in a dynamic way tied to the increasing S (as done in variations 1–6) does not improve the results when compared to variations 7–9 using a static value of θ . It seems that the increased variance in the perturbations gained by a larger θ does, especially for larger values of S , decrease the solution quality. We finally mention that in an internal test this first experiment was repeated with $p_{\max} \in \{400, 500, 600\}$ instead of $p_{\max} \in \{100, 200, 300\}$ in all nine variations. While this slightly improved the overall solution quality as expected, the comparison between the variations remains the same and variation 9 was still dominant. Therefore, we chose to not include these results in this presentation.

As a result from this first experiment we now fix $p_{\max} = 300$ and $\theta = 3$ in the IPA for the remaining experiments.

5.3.2. Second experiment. In our second experiment, we want to investigate the robustness of the IPA with respect to its stochastic component, i.e., the random choices made in Algorithm 2.b, in the chosen setting. To this end, for each value of

$S \in \{3, 6, 10, 15, 20\}$, we generate a random problem instance, i.e., a random desired state with S active sources as described in the first experiment, and solve that problem instance 100 times with the IPA. To investigate the stochastic robustness of the algorithm, we then plot for each problem instance a box-plot of the objective function values and the solution times of the respective 100 solves of the instance with the IPA. The results can be seen in Figure 3, where the first row contains the box-plots of the function values and the second row contains the box-plots of the solution times. A box-plot (as depicted in Figure 3) consists of several parts: the lower and upper end of the blue box represent the 25th and the 75th percentile of the data vector represented in the respective box-plot, the red line inside the box depicts the median of the data and the black dashed lines extending the box (especially seen in the second row of Figure 3) are the so called *whiskers* which represent the remaining data points that are not considered outliers. The outliers are then depicted as red crosses.

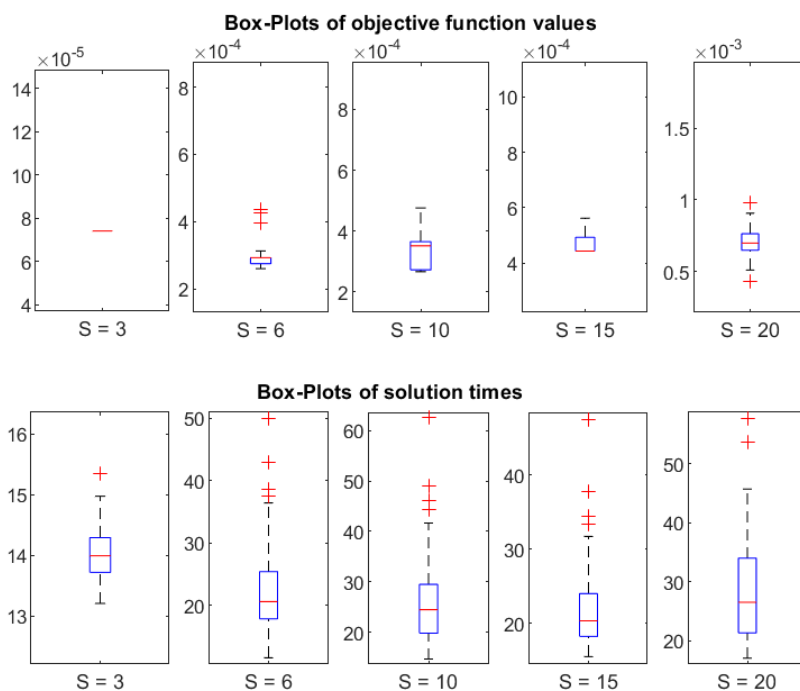


Fig. 3: Results of second experiment. Box-plots for the objective function values in the first row and box-plots for the solution times in seconds in the second row. The columns contain the plots for the problem instances with $S \in \{3, 6, 10, 15, 20\}$ active sources.

We begin with the discussion of the first row of pictures of Figure 3, i.e., the results with respect to solution quality. In the first picture, we can see that there is no variation in the function value obtained by the IPA such that there is no box and the median contains all data points, so that we conclude that each solve of the problem instances with $S = 3$ active sources resulted in the same minimum function value and the IPA is robust in this case. In the case of $S = 6$ (the second picture)

the variance of function values is very small with 3 outliers and we still conclude that the IPA is robust in that setting. For the remaining box-plots, we can see that the robustness starts to become slightly worse for an increase in S but having a look at the scale in the y-axis of these plots we can also safely say that, while different minimizers might be found by the IPA, all of them still have very high quality and should be satisfactory solutions for the respective problem instance. Having a look at the second row of pictures of Figure 3, i.e., the box-plots for the solution times, we can observe very little variance in the solution time for $S = 3$ (the first picture). Again, as S and thus the complexity of the problem increases, we can observe more variance in the solution times but it still looks very much acceptable. We also note that the overall solution time seems to increase for larger values of S which indicates that the IPA actively starts to search for better solutions via Algorithms 2.a and 2.b.

5.3.3. Third experiment. In our final third experiment we now want to compare the IPA with the solution strategies described in Section 4, i.e., the Smart Rounding, the Penalty approach from Algorithm 3 and the Branch-and-Bound routine `cplexmiqp`. In order to do so, we construct another test set as described in the first experiment and as the desired states in these test sets are randomly generated, this newly generated test set differs from the one used in the first experiment. We then solve this test set with the four algorithms in question and compare solution time and quality. In addition to the three criteria used in the first experiment ('min_count', 'rel_err_av' and 't_av'), we also report 't_min' and 't_max' the times required by an algorithm for the shortest and longest of the 100 runs of the test set corresponding to a value of S . We note that due to the different implementation languages included in this comparison, the reported computational times only give a qualitative information on the performance of the solvers. Finally, we also observe for each algorithm and each value of S 'av_active_sources', the average amount of sources that were active in the minimizers, which simply corresponds to the sum of the control. The results of this experiment can be found in Table 1.

As a first observation from this experiment, we note that `cplexmiqp` does achieve a perfect 'min_count'-score for $S = 3$ and $S = 6$ where it always find the global minimizer. Therefore, the IPA finds the global minimizer in 97 of the cases for $S = 3$ with a 5% relative error in the remaining three cases and for $S = 6$, the IPA finds the global minimizer 60 times with a relative error of around 23% in the remaining cases. While the computational time required by `cplexmiqp` is very low for $S = 3$ it is already about an order larger than the time required by the IPA for $S = 6$. So already we can see that the IPA is an interesting alternative method if one does not require a global minimizer but is satisfied with a very good local minimizer. For the remaining cases, we can observe that `cplexmiqp` starts to hit the time limit of 3600 seconds (and as internal tests have shown also the imposed memory limit) and thus terminates with a feasible solution that is vastly inferior to the solution presented by the IPA. It is also worth mentioning that the increased combinatorial complexity induced by an increase in S does only slightly increase the average solution time of the IPA. Taking the other two algorithms into consideration, we can see that the simple rounding strategy seems to not produce reliably good results in any of the cases considered. The simple penalty approach from Algorithm 3 does struggle with finding the global minimizer quite a bit but the relative average error does indicate that the solution found by the algorithm is somehow nearby the global minimizer or (for larger values of S) the solution obtained by the IPA. As the IPA is a straight improvement of Algorithm 3 this surely was expected.

$S = 3$						
	t_min	t_max	t_av	min_count	rel_err_av	av_active_sources
Smart Rounding	0.04	1.57	0.08	31	20.05	2.11
Penalty	1.85	5.70	3.84	33	1.85	2.99
IPA	9.91	31.21	16.22	97	0.06	3.00
cplexmiqp	0.13	1.08	0.71	100	0.00	3.00
$S = 6$						
	t_min	t_max	t_av	min_count	rel_err_av	av_active_sources
Smart Rounding	0.04	0.14	0.08	6	20.29	4.65
Penalty	3.06	11.32	7.37	5	1.73	5.91
IPA	10.30	57.44	22.69	60	0.23	6.00
cplexmiqp	37.19	430.67	209.69	100	0.00	6.00
$S = 10$						
	t_min	t_max	t_av	min_count	rel_err_av	av_active_sources
Smart Rounding	0.07	0.47	0.22	0	17.76	8.30
Penalty	4.63	29.68	16.55	7	1.41	9.81
IPA	11.78	154.99	31.96	83	0.25	9.98
cplexmiqp	914.13	3613.07	3272.61	14	0.71	9.98
$S = 15$						
	t_min	t_max	t_av	min_count	rel_err_av	av_active_sources
Smart Rounding	0.28	0.58	0.41	2	15.04	13.12
Penalty	21.01	42.66	31.57	5	0.95	14.62
IPA	15.71	82.76	37.41	93	0.15	14.92
cplexmiqp	786.93	3607.78	1356.60	0	1.88	14.98
$S = 20$						
	t_min	t_max	t_av	min_count	rel_err_av	av_active_sources
Smart Rounding	0.31	0.65	0.44	0	14.22	17.95
Penalty	29.07	50.42	41.12	5	0.76	19.45
IPA	17.38	136.94	42.10	95	0.22	19.81
cplexmiqp	1470.79	3602.22	2652.54	0	2.82	19.96

Table 1: Results of the third experiment. Comparison of the Smart Rounding, the Penalty approach, the IPA and `cplexmiqp` for different values of S .

From the discussed results, we can conclude that the IPA applied to this simple stationary test problem does provide encouraging results and it will be very interesting to apply the algorithm to large-scale problems such as the time-dependent variation of the model problem discussed in Remark 2.2. For these large problems it will then be indispensable to provide a local solver for Algorithm 2.a that is able to handle the resulting large linear systems efficiently.

6. Conclusion. A standard binary optimal control problem governed by a stationary PDE with a modelled control combining PDE-constrained optimization and integer programming was presented and discretized. As standard solution techniques for such problems like Branch-and-Bound are struggling for large-scale versions of such problems, an alternative solution approach via penalization was pursued. A novel Improved Penalty Algorithm (IPA) was presented. The method represents a practical implementation of an algorithmic scheme belonging to a specific family of Exact Penalty approaches. It suitably combines a local solver, a basin hopping strategy and an updating tool for the penalty parameter. Even if the developed method is for a specific class of MIPDECO problems, those techniques involved can be gen-

eralized to different model problems as well. In a numerical discussion the IPA was compared to `cplexmiqp`, the Branch-and-Bound routine of CPLEX, as well as a simple rounding strategy and a naive penalization strategy. Numerical experiments including an increased combinatorial complexity in the model problem showed encouraging results for the IPA. Future research will apply the method to large-scale problems with a time-dependent PDE as well as a time-dependent control.

Acknowledgement. D. Garmatter and M. Stoll acknowledge the financial support by the Federal Ministry of Education and Research of Germany (support code 05M18OCB). D. Garmatter, M. Porcelli, and M. Stoll were partially supported by the DAAD-MIUR Joint Mobility Program 2018-2020 (Grant 57396654). The work of M. Porcelli was also partially supported by the National Group of Computing Science (GNCS-INDAM).

REFERENCES

- [1] Ibm ilog cplex optimization studio. <https://www.ibm.com/analytics/cplex-optimizer>.
- [2] Matlab's fmincon with interior-point. <https://www.mathworks.com/help/optim/ug/constrained-nonlinear-optimization-algorithms.html#brnpd5f>. Accessed: 2019-07-09.
- [3] P. Belotti, C. Kirches, S. Leyffer, J. Linderoth, J. Luedtke, and A. Mahajan. Mixed-integer nonlinear optimization. *Acta Numerica*, 22:1–131, 2013.
- [4] C. Buchheim, R. Kuhlmann, and C. Meyer. Combinatorial optimal control of semilinear elliptic PDEs. *Computational Optimization and Applications*, 70(3):641–675, 03 2018.
- [5] M. F. P. Costa, A. M. A. C. Rocha, R. B. Francisco, and E. M. G. P. Fernandes. Firefly penalty-based algorithm for bound constrained mixed-integer nonlinear programming. *Optimization*, 65(5):1085–1104, 01 2016.
- [6] M. De Santis and F. Rinaldi. Continuous reformulations for zero–one programming problems. *Journal of Optimization Theory and Applications*, 153(1):75–84, 2012.
- [7] G. Di Pillo, S. Lucidi, and F. Rinaldi. An approach to constrained global optimization based on exact penalty functions. *Journal of Global Optimization*, 54(2):251–260, 2012.
- [8] S. R. Fipke and A. O. Celli. The use of multilateral well designs for improved recovery in heavy-oil reservoirs. In *IADC/SPE Drilling Conference*. Society of Petroleum Engineers, 2008.
- [9] S. Funke, P. Farrell, and M. Piggott. Tidal turbine array optimisation using the adjoint approach. *Renewable Energy*, 63:658 – 673, 2014.
- [10] F. Giannessi and F. Niccolucci. Connections between nonlinear and integer programming problems. In *Symposia Mathematica*, volume 19, pages 161–176. Academic Press New York, 1976.
- [11] F. Giannessi and F. Tardella. Connections between nonlinear programming and discrete optimization. In *Handbook of Combinatorial Optimization*, pages 149–188. Springer US, 1998.
- [12] S. Göttlich, A. Potschka, and C. Teuber. A partial outer convexification approach to control transmission lines. *Computational Optimization and Applications*, 72(2):431–456, 03 2019.
- [13] A. Grosso, M. Locatelli, and F. Schoen. A population-based approach for hard global optimization problems based on dissimilarity measures. *Math. Program.*, 110(2):373–404, 2007.
- [14] M. Hahn, S. Leyffer, and V. M. Zavala. Mixed-integer pde-constrained optimal control of gas networks. *Techreport*. url: <https://wiki.mcs.anl.gov/leyffer/images/2/27/GasNetMIP.pdf> (visited on 06/25/2018), 2017.
- [15] J. Larson, S. Leyffer, P. Palkar, and S. M. Wild. A method for convex black-box integer global optimization. *arXiv preprint arXiv:1903.11366*, 2019.
- [16] R. H. Leary. Global optimization on funneling landscapes. *J. Global Optim.*, 18(4):367–383, 2000.
- [17] S. Leyffer. *Optimization: Applications, algorithms and computations: 24 lectures on nonlinear optimization and beyond*, 2016.
- [18] M. Locatelli and F. Schoen. *Global optimization: theory, algorithms, and applications*, volume 15. Siam, 2013.
- [19] S. Lucidi and F. Rinaldi. Exact penalty functions for nonlinear integer programming problems. *Journal of Optimization Theory and Applications*, 145(3):479–488, 04 2010.
- [20] S. Lucidi and F. Rinaldi. An exact penalty global optimization approach for mixed-integer

- programming problems. *Optimization Letters*, 7(2):297–307, 10 2011.
- [21] P. Manns and C. Kirches. Multi-dimensional sum-up rounding for elliptic control systems. *DFG Preprint SPP1962-080*, 2018.
- [22] W. Murray and K.-M. Ng. An algorithm for nonlinear optimization problems with binary variables. *Computational Optimization and Applications*, 47(2):257–288, 12 2008.
- [23] U. Ozdogan and R. N. Horne. Optimization of well placement under time-dependent uncertainty. *SPE Reservoir Evaluation & Engineering*, 9(02):135–145, 04 2006.
- [24] M. E. Pfetsch, A. Fügenschuh, B. Geißler, N. Geißler, R. Gollmer, B. Hiller, J. Humpola, T. Koch, T. Lehmann, A. Martin, et al. Validation of nominations in gas network optimization: models, methods, and solutions. *Optimization Methods and Software*, 30(1):15–53, 2015.
- [25] G. D. Pillo, S. Lucidi, and F. Rinaldi. A derivative-free algorithm for constrained global optimization based on exact penalty functions. *Journal of Optimization Theory and Applications*, 164(3):862–882, 11 2013.
- [26] F. Rinaldi. New results on the equivalence between zero-one programming and continuous concave programming. *Optimization Letters*, 3(3):377–386, 03 2009.
- [27] F. Tröltzsch. *Optimal control of partial differential equations: theory, methods, and applications*, volume 112. American Mathematical Soc., 2010.
- [28] C. Wesselhoeft. *Mixed-Integer PDE-Constrained Optimization*. PhD thesis, Imperial College London, 2017.
- [29] P. Y. Zhang, D. A. Romero, J. C. Beck, and C. H. Amon. Solving wind farm layout optimization with mixed integer programs and constraint programs. *EURO Journal on Computational Optimization*, 2(3):195–219, 08 2014.
- [30] W. Zhu. Penalty parameter for linearly constrained 0–1 quadratic programming. *Journal of Optimization Theory and Applications*, 116(1):229–239, 2003.